Draft version May 2, 2024
Typeset using LaTeX **twocolumn** style in AASTeX631

Analyzing eROSITA Sources as Potential LISA Progenitors

Azeem Bari[1] and Sofía Martínez Fortis[1]

[1] *Vanderbilt University*

ABSTRACT

The rise of gravitational astronomy is not the demise of EM astronomy, as both practices complement each other. Observing both the gravitational and electromagnetic waves of the same source allows the study of binary systems long before, shortly before, during, and after the merger, as well as constraining the sky localization of the source. LISA, which is expected to launch in 2034, will detect gravitational waves (GWs) from merging massive black hole binaries (MBHBs) with masses ranging from 10^4 to 10^8 $M_\odot$ and frequencies of $\sim 10^{-4}$ Hz to a few Hz. The eROSITA survey enables a deeper study of X-ray-emitting active galactic nuclei (AGNs) that are possibly in a binary orbit within the LISA mass range. We analyze eROSITA hard X-ray sources from its first data release (eRASS1) as potential LISA progenitors by computing their mass-redshift relationship and comparing it to LISA's mass-redshift constraints at varying signal-to-noise ratios (SNRs). We find that most eROSITA sources can accumulate $SNR > 8$ if observed with LISA, making them likely LISA progenitors if they are MBHBs.

1. INTRODUCTION

The development of gravitational wave (GW) detectors in the past decade has created a new field of observational astronomy in which we are able to observe the effects of general relativity directly. Though informative on its own, gravitational astronomy was not developed to replace electromagnetic (EM) astronomy, but rather to complement it. Astronomers now have the opportunity to observe a source by means of both electromagnetic and gravitational waves (Abbott et al. 2017). Multi-messenger astronomy (MMA) is a growing field as more EM and GW detectors are being developed that will provide insight into the nature of compact objects and the history of our universe. MMA observations of massive black hole binary (MBHB) mergers provide a holistic view of their evolution, as each messenger reveals different properties at different timescales. EM observations provide a tight relationship between the central black hole's (BHs) growth and key host galaxy properties (Kormendy & Ho 2013). GW detections are not only direct evidence of MBHB mergers, but they constrain the mass, mass ratio, spin, and luminosity distance of the source. MBHBs could be binary active galactic nuclei (AGN), as they may result from galaxy mergers, which provide gas-rich conditions (Lops et al. 2023). Therefore, binary AGNs are appropriate MMA candidates, as they emit gravitational and electromagnetic signatures. The study of such sources may enrich our understanding of supermassive black holes (SMBHs), as MBHs are thought to be SMBH seeds (Greene et al. 2020). X-ray observations of inspiraling MBHs will illuminate (quite literally) the violently changing spacetime around BHs prior to the merger and show how it affects light and matter, while GW observations may allow measurements of the speed of gravity in comparison to the speed of light with precision of up to 10^{-17} (Piro et al. 2022).

The Laser Interferometer Space Antenna (LISA) is a space-based mission expected to launch in 2034. LISA will detect gravitational waves emitted from MBHB merger ($\sim 10^4 - \sim 10^8\,M_\odot$) events up to redshift $z \sim 20$ (Amaro-Seoane et al. 2023). LISA may detect several MBHBs of mass $M \geq 3 \times 10^5\,M_\odot$ at redshift $z < 2$ (Piro et al. 2022).

The eROSITA (extended Roentgen Survey with an Imaging Telescope Array; (Merloni et al. 2024)) mission, on board the Spektrum Roentgen Gamma (SRG; Sunyaev, R. et al. (2021)) orbital observatory, was launched in 2019 and provides the first all-sky survey in the 0.8-2 keV band. On January 31st, 2024, the German eROSITA Consortium (eROSITA-DE) made public the first six months of the SRG/eROSITA all-sky survey (eRASS1) data (Merloni et al. 2024). Compared to all previous all-sky X-ray surveys, eROSITA has better flux, energy coverage, and resolution. Although the primary science goal of eROSITA is to map the large-scale structure of the universe in the X-ray (Merloni et al. 2012), the most prevalent sources it will detect will be AGN.

AGN emit across all wavelengths, from radio to γ, however, probing the X-ray allows for a better under-

standing of these objects given the proximity of the X-ray emission to the BH (Elvis et al. 1978). This X-ray emission is thought to be from UV photons being up-scattered in the accretion disk due to Compton collisions in a corona of relativistic electrons (Haardt & Maraschi (1991), Merloni et al. (2000), Fabian et al. (2004)). This Comptonization results in an X-ray spectrum that takes the form of a power law, with a high-energy turnaround at a few hundred keV (Petrucci et al. (2001), Fabian et al. (2015)) that corresponds to the temperature and optical depth of the electrons in the corona, and a low-energy turnaround of ∼1 eV (Shakura & Sunyaev 1973) that corresponds to the temperature of UV photons in the inner accretion disk.

However, in the case of a GW signal being accompanied by an EM signal, the AGN has to be a binary AGN. Not to be confused with dual AGN, which are a pair of AGN with kiloparsec-scale separations, binary AGN are a pair of BHs that are gravitationally bound with separations typically < 100 pc (Foord et al. 2019). It is expected that, with a sufficient amount of gas accreting onto the binary, an EM counterpart will be triggered during inspiral, merger, or ringdown (see Mangiagli et al. (2022) and references within). Additionally, each phase will exhibit its own distinct spectral features.

In this letter, we analyze the likelihood of eROSITA sources being LISA progenitors. We limited our study to hard-only point sources in the first all-sky survey and assumed they were all binary AGN. In Section 2, we provide our methodology for selecting the eROSTIA sources and simulating the LISA SNR curves. We present our results in Section 3 and discuss them in Section 4 before summarizing in Section 5. Throughout this paper, we assume a ΛCDM cosmology with $\Omega_m = 0.3$, $\Omega_\Lambda = 0.7$, and $\Omega_b = 0.048$.

2. METHODOLOGY

2.1. *Selection Criteria of eROSTIA Sources*

We describe below our method of selecting potential hard X-ray emitting AGN binaries in the eRASS1 all-sky survey in the western galactic sky. The hard (2.3 - 5 keV) X-ray selected catalog we use is presented in (Merloni et al. 2024) and contains a total of 5466 sources. However, to eliminate any soft X-ray-emitting contaminants, we select hard-only sources. As defined in (Waddell et al. 2024), hard-only sources are selected by:

$$\text{DET\_LIKE\_1} < 5 \,\&\, \text{DET\_LIKE\_2} < 5 \tag{1}$$

where 1 indicates the 0.2-0.6 keV band and 2 indicates the 0.6-2.3 keV band. This criterion rejects sources that have detection likelihoods in either band equal to the soft X-ray sample cutoff (Waddell et al. 2024) at DET_LIKE_0> 5 (where 0 indicates the 0.2-2.3 keV band). In total, 738 sources meet this requirement. In addition, since we expect these AGN binaries to be point sources in the X-ray, we require that:

$$\text{EXT\_LIKE (extended likelihood)} = 0 \tag{2}$$

with both criteria applied, we have a total of 719 hard-only point sources.

Since eROSITA only measures the X-ray flux in each band, we have to estimate the masses of these potential AGN binaries by allowing them to reside over a range of redshifts. We choose to range these sources over $0.01 < z < 10$, as motivated by our LISA SNR curve. This range gives these potential MBHBs the highest chance of being detected by LISA.

First, we estimate the rest X-ray luminosity of these sources used by Runnoe et al. (2012):

$$L_X = \frac{4\pi d_l^2 f_X}{1+z} \tag{3}$$

where d_l is the luminosity distance, f_X is the flux in the 2.3 - 5 keV band, and z is the redshift of the object. Following eq. 3, we estimate the bolometric luminosity to be:

$$L_{bol} = \text{BC} \cdot L_X \tag{4}$$

where BC is the bolometric correction. Given the bolometric luminosity and assuming an accretion rate, we can then estimate the total BH binary mass:

$$\begin{aligned} L_{Edd} &= \frac{L_{bol}}{\lambda_{Edd}} \\ M_{MBHB} &= \frac{L_{Edd}}{3.2 \times 10^4 L_\odot} \end{aligned} \tag{5}$$

in units of $M_\odot$. We assume a BC of 10 given the hard X-ray nature of these sources (Vasudevan et al. 2009) and assume the MBHB is accreting at the Eddington limit, i.e. $\lambda_{Edd} = 1$.

2.2. *Simulating LISA SNR Curves*

We use the python module, *pycbc* to simulate LISA-like waveforms, power spectral density functions, and to compute the signal-to-noise ratio. The input parameters we use to obtain the waveform are shown in the table below where f_{min} is the minimum frequency, f_{max} is the maximum frequency, Δf is the step size in between measurements, and d is the distance at which $z = 0$. We assume a mass range between 10 and 10^9 $M_\odot$ and a spin of 0 for each individual BH.

f_{min} (Hz)	f_{max} (Hz)	Δf (Hz)	**d** (Mpc)
2×10^{-5}	0.5	10^{-4}	100

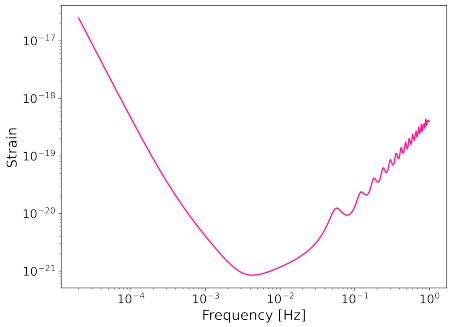

Figure 1. Noise curve for LISA

We calculate the horizon distance, d_h using the following formula,

$$d_h = d\frac{SNR}{SNR_{scale}} \tag{6}$$

where d is the distance at which $z = 0$, SNR is the signal-to-noise ratio, and SNR_{scale} is the minimum signal-to-noise ratio we aim to obtain. Then, we compute the corresponding redshift using the python module, *astropy*, assuming cosmology parameters of those in (Planck Collaboration et al. 2020). Lastly, we calculate the source mass, M_{source} as follows,

$$M_{source} = \frac{M_{det}}{z+1} \tag{7}$$

where M_{det} is the total mass detected.

3. RESULTS

In this section, we present the sample of potential hard-only X-ray emitting binary AGN in the eROSITA catalog and the results from simulating LISA SNR curves. The sky positions of the hard-only point-like eROSITA sources are shown in Fig. 2. Additionally, Fig. 2 shows the range of fluxes these sources exhibit in the hard band, from 10^{-15} to 5 $\times 10^{-13}$ erg/s/cm^2/Å.

As binaries can exhibit a range of mass ratios (q), we focus on the two scenarios where the mass ratios of the binaries are 0.1 and 1. Given that each of the 719 hard X-ray sources has a range of possible redshifts and masses as opposed to one value for each, we present them by means of a two-dimensional histogram (Fig. 3) to visualize the distribution of all of the possible mass-redshift relationships based on our model (see equations 3, 4, and 5). Each of the pink SNR curves in Figure 3 represents the redshift and mass boundaries necessary to achieve the desired SNR if observed by LISA. Therefore, any sources plotted below a particular SNR curve are able to accumulate the desired SNR.

4. DISCUSSION

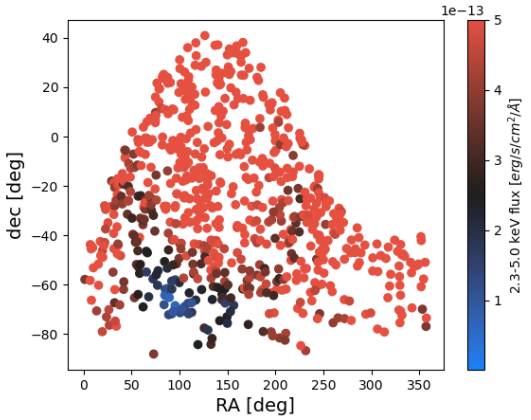

Figure 2. Sky positions of hard-only point-like X-ray sources in eRASS1. The color corresponds to the hard band (2.3-5 keV) flux

As expected, the $SNR = 8$ curves encapsulate more data than the $SNR = 4096$ curves, since it is more likely for sources to produce a minimum SNR of 8 than of 4096. In the case of q = 0.1, achieving SNRs $\geq$ 256 requires that an eROSITA source is $z \lesssim 1$, but allows the detection of most masses at that redshift. Conversely, the equal-mass case allows a wider redshift range but is limited in mass. These caveats are better depicted in Figure 4 where we analyze LISA's detectability of the mass distribution of our eROSITA sources within 10% of redshifts $z = 0.5$, 1, and 1.5, assuming mass ratios q = 0.1 and q = 1. By doing so, we analyze LISA's capabilities of observing MBHBs near its upper mass limit, as the mass distribution at such redshifts exceeds $10^{6.5}$ M$_\odot$. We find that for LISA to observe large masses, a low redshift is favored.

4.1. $z = 0.5 \pm 0.05$

In the case where $z \approx 0.5$, the most probable mass is about $10^{7.5}$ M$_\odot$. For q=0.1, most of the mass distribution is able to accumulate an SNR of at least 1024, while in the q=1 case, the majority of the mass can accumulate an SNR of 4096 if observed by LISA. This is the most optimistic scenario, as high SNRs are likely regardless of mass ratio.

4.2. $z = 1 \pm 0.1$

In the case where $z \approx 1$, the most probable mass is about $10^{8.13}$ M$_\odot$. In the unequal mass case, an SNR of 64 is plausible, though the mass threshold for such is slightly lower than the most probable mass. The equal mass scenario is significantly more optimistic, as most of the mass distribution at this redshift falls under the SNR=256 threshold.

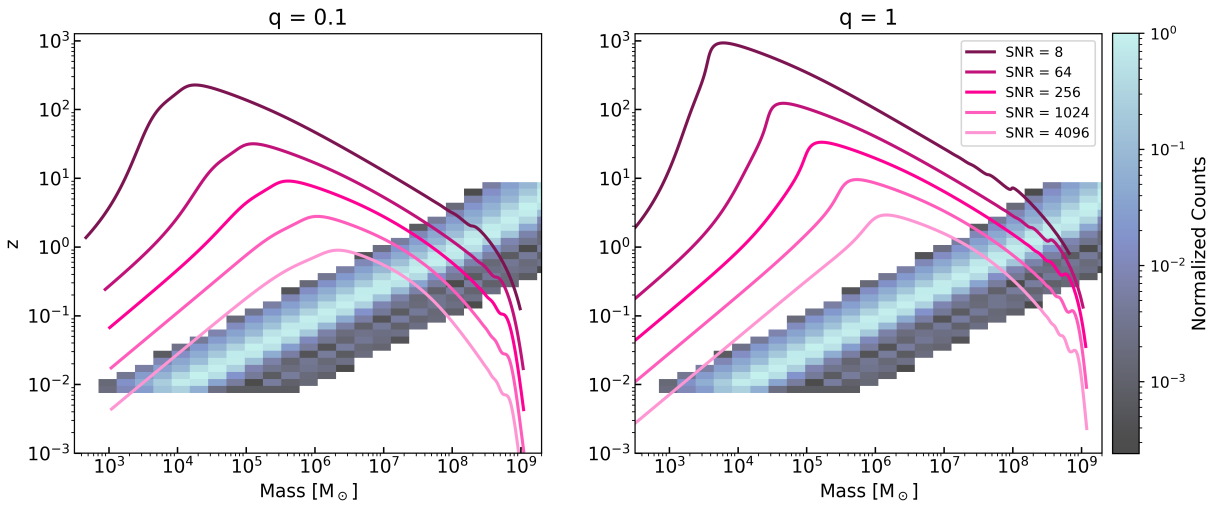

Figure 3. The two-dimensional histogram depicts the mass and redshift distribution of the eROSITA binaries. The pink curves illustrate the redshift necessary to achieve the desired SNR as a function of mass for a low mass ratio as shown in the left panel, and an equal mass ratio as depicted in the right panel. The SNR curves are the only differences between the panels, as the redshift-mass distribution of eROSITA sources is independent of mass ratio.

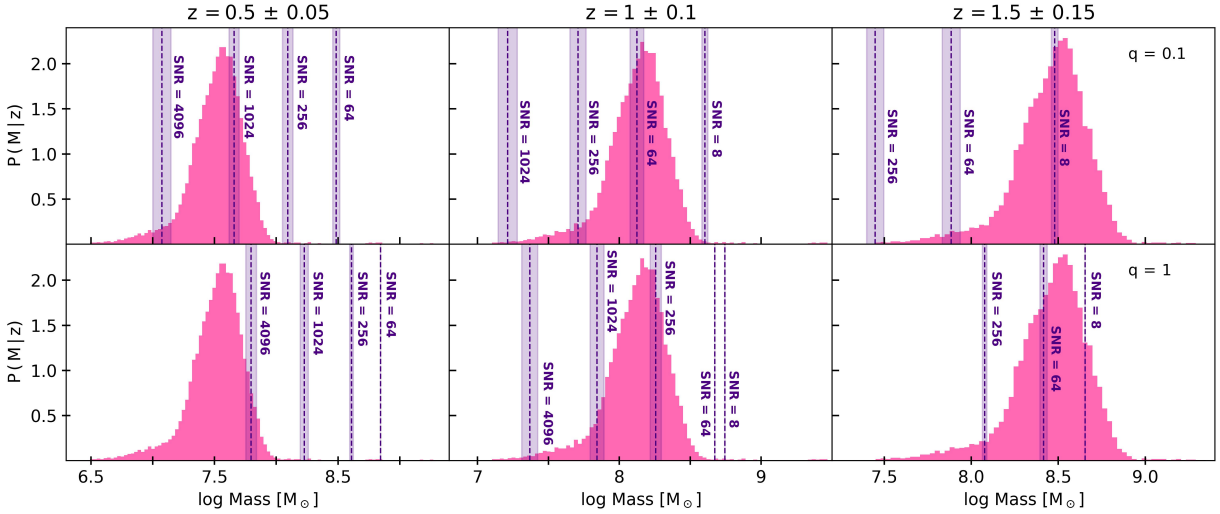

Figure 4. The pink histograms illustrate the mass distribution at redshifts within 10% of $z = 0.5$, 1, and 1.5. The indigo lines mark the mass at $z \pm 10\%$ needed to achieve each target SNR given that the mass ratio is q = 0.1 (top panels) or q = 1 (bottom panels).

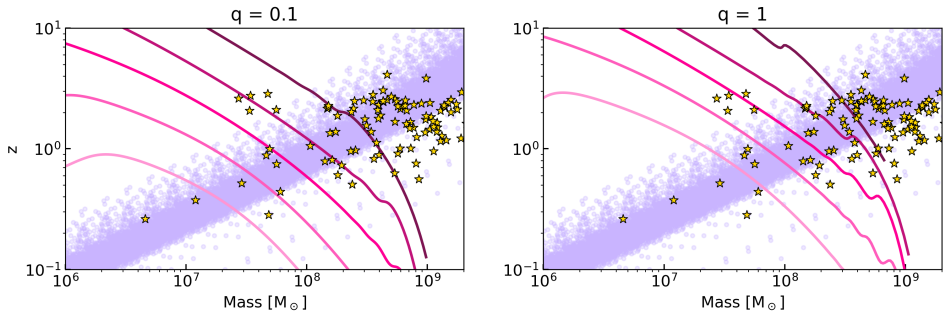

Figure 5. Zoomed in plot of the mass distribution of the hard-only eROSITA point sources (purple) cross-matched to SDSS DR16q quasars (stars) for mass ratios of 0.1 (left) and 1 (right). The LISA SNR curves are overplotted in pink.

4.3. $z = 1.5 \pm 0.15$

In the case where $z \approx 1.5$, the most probable mass is about $10^{8.46}$ $M_\odot$, which resides at the upper boundary of

masses LISA can observe, if at all. Assuming that LISA can detect such masses, an MBHB system with an equal mass ratio is likely to accumulate an SNR of at least 8. The probability of such a system accumulating an SNR of 64 is less than half based on the mass distribution, though it is high enough that it should not be ignored.

In the case where q = 0.1, accumulating an SNR of 8 has a probability of $\sim 50\%$, assuming the binary is accreting at the Eddington limit.

4.4. *Cross-match With SDSS*

To ensure our X-ray sources are emitted by AGN activity and not stars, we cross-match our hard-only eROSITA point sources to SDSS DR16q (Wu & Shen 2022) quasars to within 10 arc-minutes. We overplot the redshift of the cross-matched SDSS quasars with the hard-only eROSITA point sources as a function of mass in Fig. 5. Taking into account different mass ratios, the left panel shows the distribution with LISA SNR curves for q = 0.1 and the right panel for q = 1.

Comparing the cross-matched SDSS DR16q quasars to our eROSITA sources, we see a large fraction of them overlap. Furthermore, for both mass ratios, most of the SDSS quasars lie outside SNR = 8. However, this is expected from DR16q since the quasars targeted in that survey were chosen to be the brightest sources. Hence, despite this anticipated bias, a significant portion of these quasars remain viable MBHB candidates that can be observed with LISA, with either mass ratio scenario. Moreover, we can cross-match our hard-only X-ray sample to confirmed star spectra, in addition to other quasar catalogs. This would allow for a more robust selection of sources and help remove extraneous X-ray sources.

4.5. *Caveats*

It should be noted that adding K corrections to the X-ray data will be required in the future to obtain more accurate results. Due to the expansion of the universe, one must correct for the quantity of light of a source at redshift z to the source's restframe. With the correction applied, we expect the corrected fluxes to be higher than the ones reported here as a function of redshift. Therefore, the masses will be larger as redshift increases.

Additionally, the rate at which the BH is accreting affects its total mass. We chose the most conservative estimate and considered the BH is accreting at the Eddington limit. However, if these MBHBs were accreting at sub-Eddington limits, their masses would also increase.

When selecting for binary AGN with photometric data, contaminants are likely to populate the selection. In the case of the hard X-ray band, X-ray binaries are the biggest interlopers, with positive hardness ratios in hard bands and X-ray luminosities reaching $\sim 10^{39} - 10^{40}\,\mathrm{erg\,s^{-1}}$. To select these out of our selection, we can apply a criterion that only allows for sources with $L_X > 10^{40}\,\mathrm{erg\,s^{-1}}$ to exist within the sample. This would increase the likelihood that we are selecting only AGNs that are potential LISA progenitors.

5. SUMMARY AND CONCLUSIONS

As we prepare for the advent of LISA, we study binary AGN as potential MMA candidates. Specifically, we explored the possibility of eROSITA hard X-ray sources being LISA progenitors. We found that for these sources, such detections are plausible at $z \lesssim 1.5 \pm 0.15$, favoring a low redshift. Additionally, binaries with equal-mass black holes are likely to accumulate higher SNRs than those with unequal masses. The best case scenario for observing eROSITA sources with LISA is if they are at $z \lesssim 0.5$ and have a mass ratio of q = 1, as they have an SNR of 4096. The case where such an MMA observation is the least plausible is that in which the binary's mass ratio is q = 0.1 and the source is at $z \sim 1.5$, as the possibility of accumulating an SNR of 8 is less than half.

The findings of this project are meant to provide astronomers with a rough estimate of whether or not hard X-ray sources, like those in eROSITA, make appropriate MBHB candidates observable with LISA. However, there is not enough evidence to support the specific quantitative findings of this project, given the amount of assumptions that were made. The mass-redshift relationship derived in this project assumes that all hard X-ray sources from eRASS1 are inspiraling binary AGN that accrete at the Eddington ratio. On the LISA portion, this work assumes that the MBHBs are non-spinning, are not inclined, and are 100 Mpc away. Nevertheless, the results presented in this paper support our claim that eROSITA sources are promising LISA progenitor candidates.

In order to make more conclusive statements, analyzing X-ray variability in time-series data would be required. Looking for key signatures in the variability would not only help distinguish between stars and AGN but also help to identify if the source is an MBHB. This could be done by comparing our data to archival X-ray data to make a light curve. Also, accessing the eSASS srctool (Merloni et al. 2024) will allow for analyzing light curves of eROSITA sources, as well as confirming sources with spectra. Follow-up with future eROSITA data releases will allow for studying X-ray variability for millions of sources with months/year timescales.

Overall, our conclusions are not limited to eROSITA data. We suggest that other X-ray surveys may be ap-

propriate counterparts to LISA's future observations, which will help solidify future MMA MBHB studies.

REFERENCES

Abbott, B. P., Abbott, R., Abbott, T. D., et al. 2017, Phys. Rev. Lett., 119, 161101, doi: 10.1103/PhysRevLett.119.161101

Amaro-Seoane, P., Andrews, J., Arca Sedda, M., et al. 2023, Living Reviews in Relativity, 26, doi: 10.1007/s41114-022-00041-y

Elvis, M., Maccacaro, T., Wilson, A. S., et al. 1978, MNRAS, 183, 129, doi: 10.1093/mnras/183.2.129

Fabian, A. C., Lohfink, A., Kara, E., et al. 2015, MNRAS, 451, 4375, doi: 10.1093/mnras/stv1218

Fabian, A. C., Miniutti, G., Gallo, L., et al. 2004, Monthly Notices of the Royal Astronomical Society, 353, 1071, doi: 10.1111/j.1365-2966.2004.08036.x

Foord, A., Gültekin, K., Reynolds, M. T., et al. 2019, ApJ, 877, 17, doi: 10.3847/1538-4357/ab18a3

Greene, J. E., Strader, J., & Ho, L. C. 2020, Annual Review of Astronomy and Astrophysics, 58, 257, doi: 10.1146/annurev-astro-032620-021835

Haardt, F., & Maraschi, L. 1991, ApJL, 380, L51, doi: 10.1086/186171

Kormendy, J., & Ho, L. C. 2013, ARA&A, 51, 511, doi: 10.1146/annurev-astro-082708-101811

Lops, G., Izquierdo-Villalba, D., Colpi, M., et al. 2023, Monthly Notices of the Royal Astronomical Society, 519, 5962–5986, doi: 10.1093/mnras/stad058

Mangiagli, A., Caprini, C., Volonteri, M., et al. 2022, Physical Review D, 106, doi: 10.1103/physrevd.106.103017

Merloni, A., Fabian, A. C., & Ross, R. R. 2000, MNRAS, 313, 193, doi: 10.1046/j.1365-8711.2000.03226.x

Merloni, A., Predehl, P., Becker, W., et al. 2012, eROSITA Science Book: Mapping the Structure of the Energetic Universe. https://arxiv.org/abs/1209.3114

Merloni, A., Lamer, G., Liu, T., et al. 2024, A&A, 682, A34, doi: 10.1051/0004-6361/202347165

Petrucci, P. O., Haardt, F., Maraschi, L., et al. 2001, ApJ, 556, 716, doi: 10.1086/321629

Piro, L., Ahlers, M., Coleiro, A., et al. 2022, Experimental Astronomy, 54, 23–117, doi: 10.1007/s10686-022-09865-6

Planck Collaboration, Aghanim, N., Akrami, Y., et al. 2020, A&A, 641, A6, doi: 10.1051/0004-6361/201833910

Runnoe, J. C., Brotherton, M. S., & Shang, Z. 2012, Monthly Notices of the Royal Astronomical Society, 426, 2677, doi: 10.1111/j.1365-2966.2012.21644.x

Shakura, N. I., & Sunyaev, R. A. 1973, A&A, 24, 337

Sunyaev, R., Arefiev, V., Babyshkin, V., et al. 2021, AA, 656, A132, doi: 10.1051/0004-6361/202141179

Vasudevan, R. V., Mushotzky, R. F., Winter, L. M., & Fabian, A. C. 2009, Monthly Notices of the Royal Astronomical Society, 399, 1553, doi: 10.1111/j.1365-2966.2009.15371.x

Waddell, S. G. H., Buchner, J., Nandra, K., et al. 2024, arXiv e-prints, arXiv:2401.17306, doi: 10.48550/arXiv.2401.17306

Wu, Q., & Shen, Y. 2022, The Astrophysical Journal Supplement Series, 263, 42, doi: 10.3847/1538-4365/ac9ead